

Time-Resolved Delayed Luminescence Image Microscopy Using an Europium Ion Chelate Complex

Gerard Marriott,* Manfred Heidecker,* Eleftherios P. Diamandis,[†] and Yuling Yan-Marriott*

*Department of Cell Biology, Max Planck Institute for Biochemistry, 82152 Martinsried bei München, Germany, and [†]Department of Clinical Biochemistry, The Toronto Hospital, Toronto Western Division and Department of Clinical Biochemistry, University of Toronto, Ontario, Canada

ABSTRACT Improvements and extended applications of time-resolved delayed luminescence imaging microscopy (TR-DLIM) in cell biology are described. The emission properties of europium ion complexed to a fluorescent chelating group capable of labeling proteins are exploited to provide high contrast images of biotin labeled ligands through detection of the delayed emission. The streptavidin-based macromolecular complex (SBMC) employs streptavidin cross-linked to thyroglobulin multiply labeled with the europium-fluorescent chelate. The fluorescent chelate is efficiently excited with 340-nm light, after which it sensitizes europium ion emission at 612 nm hundreds of microseconds later. The SBMC complex has a high quantum yield orders of magnitude higher than that of eosin, a commonly used delayed luminescent probe, and can be readily seen by the naked eye, even in specimens double-labeled with prompt fluorescent probes. Unlike triplet-state phosphorescent probes, sensitized europium ion emission is insensitive to photobleaching and quenching by molecular oxygen; these properties have been exploited to obtain delayed luminescence images of living cells in aerated medium thus complementing imaging studies using prompt fluorescent probes. Since TR-DLIM has the unique property of rejecting enormous signals that originate from scattered light, autofluorescence, and prompt fluorescence it has been possible to resolve double emission images of living amoeba cells containing an intensely stained lucifer yellow in pinocytosed vesicles and membrane surface-bound SBMC-labeled biotinylated concanavalin A. Images of fixed cells represented in terms of the time decay of the sensitized emission show the lifetime of the europium ion emission is sensitive to the environment in which it is found. Through the coupling of SBMC to streptavidin, a plethora of biotin-based tracer molecules are available for immunocytochemical studies.

INTRODUCTION

In time-resolved delayed luminescence imaging microscopy (TR-DLIM) the long-lived emission of the luminescent probe is exploited to reject background signals such as cellular autofluorescence and Rayleigh and Raman scatter (Marriott et al., 1991). Detection of the delayed emission leads to an increase in the signal-to-noise ratio of the probe, thereby improving image contrast, lowering the detection limit of the probe, as well as providing a time-resolved method to separate the emission of multiple probes in a mixture (Marriott et al., 1991). Despite these positive features, TR-DLIM is rarely used in cell biology, presumably because of the low phosphorescence quantum efficiency of triplet-state probes, which is often hundreds of times less than the fluorescence quantum yield of prompt fluorescence probes. Additionally, triplet-state-based imaging normally requires oxygen-free buffers, a condition incompatible with studies on most living cells. To overcome these limitations, we are investigating the use of fluorescent labeling reagents capable of chelating europium ions and sensitizing its emission. Eu-

ropium ion emission is long-lived and insensitive to oxygen quenching, but the hydrated ion has a poor extinction coefficient and weak emission. Europium ions, however, can be complexed in certain fluorescent chelates which replace water ligands and through excitation of the fluorophore, which has a high extinction coefficient, an efficient sensitized emission of the europium ion may occur (Saha et al., 1993). Herein we show that the fluorescent, europium ion chelate protein-labeling reagent, 4,7-bis(chlorosulfonyl)-1,10-phenanthroline-2,9-dicarboxylic acid (BCPDA), described by Evangelista et al. (1988), is a very effective probe for TR-DLIM. Europium ions bind to BCPDA with a dissociation constant of about $4 \times 10^{-8} \text{ M}^{-1}$ (Gudgin Templeton and Pollak, 1989). Eu^{3+} is not displaced by the divalent ions commonly found in biological tissue (Evangelista et al., 1988) and upon excitation of the bathophenanthroline group between 320 and 350 nm, an efficient energy transfer process occurs which sensitizes europium ion emission at 612 nm. The lifetime of the sensitized emission is from 210 to 770 μs , depending on the stoichiometry of the Eu^{3+} -BCPDA complex and buffer conditions (Gudgin Templeton and Pollak, 1989). An extremely sensitive analytical reagent has also been described (Morton and Diamandis, 1990) in which about 150 BCPDA molecules are covalently attached to thyroglobulin, which is then covalently cross-linked to streptavidin; upon warming, further cross-linking to excess BCPDA-thyroglobulin can occur in the presence of europium ions, mediated by the formation of a large number of 1:2 Eu^{3+} -BCPDA complexes. This complex, known as the streptavidin-based molecular complex (SBMC) has been

Received for publication 23 March 1994 and in final form 6 June 1994.

Address reprint requests to Dr. Gerard Marriott, Department of Cell Biology, Max Planck Institute for Biochemistry, 82152 Martinsried bei München, Germany, Tel: 49-89-85-78-2314; Fax: 49-89-85-78-3777.

Abbreviations used: TR-DLIM, time-resolved delayed luminescence imaging microscopy; SBMC, streptavidin-based molecular complex; BCPDA, 4,7-bis(chlorosulfonyl)-1,10-phenanthroline-2,9-dicarboxylic acid; Con A, concanavalin A.

© 1994 by the Biophysical Society

0006-3495/94/09/957/09 \$2.00

used in time-resolved delayed fluorescence immunoassays to detect protein antigens in serum at a concentration down to 10^{-12} M (Morton and Diamandis, 1990). In this study we exploit the spectroscopic and indirect antigen labeling properties of SBMC for use as a probe in a TR-DLIM study of living and fixed cells. Recently two other europium ion complexes of fluorescent chelating groups have been applied to delayed luminescence microscopy of cells (Seveus et al., 1992; Lief and Vallarino, 1991) as well as an inorganic phosphor crystal (Beverloo et al., 1992). The europium ion-chelate probe described by Seveus et al. (1992) was used for delayed luminescence in situ hybridization with fixed cells, but it was found to be unstable during exposure to near-ultraviolet excitation light, and long exposure times were required. The europium ion chelate probe introduced by Lief and Vallarino (1991) requires a two-stage formation of a bidentate complex; applications of this probe in TR-DLIM have not been presented.

MATERIALS AND METHODS

Europium chloride was purchased from Aldrich, and aminodextran was from Molecular Probes (Eugene, OR). All other proteins and reagents were purchased from Sigma unless otherwise noted and were of the highest available grade. BCPDA was prepared according to Evangelista et al. (1988).

Protein labeling conditions

Goat anti-mouse IgG or concanavalin A (Con A) was dialyzed against 0.1 M sodium phosphate buffer pH 7.5 at 20°C and mixed with a 10-fold molar excess of biotinamidocaproyl-*N*-hydroxysuccinimide ester (Molecular Probes) for 2 h at room temperature. Unreacted biotin was removed from the protein conjugate by chromatography on a G-25 column equilibrated in 0.1 M sodium phosphate buffer, pH 7.5. The peak protein fraction was identified and quantitated by absorption at 280 nm, after which it was aliquoted and stored at -20°C. Aminodextran was labeled with a 10-molar excess of BCPDA (relative to the amino group content) using a procedure similar to that described by Diamandis and Morton (1988). SBMC was

either purchased from Cyberfluor Inc. (Toronto, Canada) and shipped on ice or prepared according to Morton and Diamandis (1990) in Toronto and shipped by regular mail. Samples not shipped on ice showed noticeable light scattering. Before use all SBMC solutions were centrifuged at 10,000 rpm in a Sorvall SS34 rotor for 30 min to remove insoluble protein. From an absorption spectrum of one of these clarified solutions, we calculated a BCPDA concentration of 135 μ M using an extinction coefficient of 15,200 $M^{-1}cm^{-1}$ (Evangelista et al., 1988) which, giving a labeling ratio of 450/1 (Morton and Diamandis, 1990), one can calculate a streptavidin concentration of ~ 0.30 μ M.

Labeling AX-2 cells with a biotin Con A conjugate

AX-2 cells were grown to a density of 5×10^6 /ml in HL-5 medium, washed with Sorensen's buffer, pH 6.5 (PB) and plated on acid-washed coverslips. After 30 min adherent cells were washed with PB, treated with 100 μ l of a 5 μ M solution of biotinylated Con A for 10 min, washed with PB, and then incubated with SBMC at a 1/5 dilution in PB. After 20 min, cells were washed with PB and then observed in the time-resolved microscope as described in a later section.

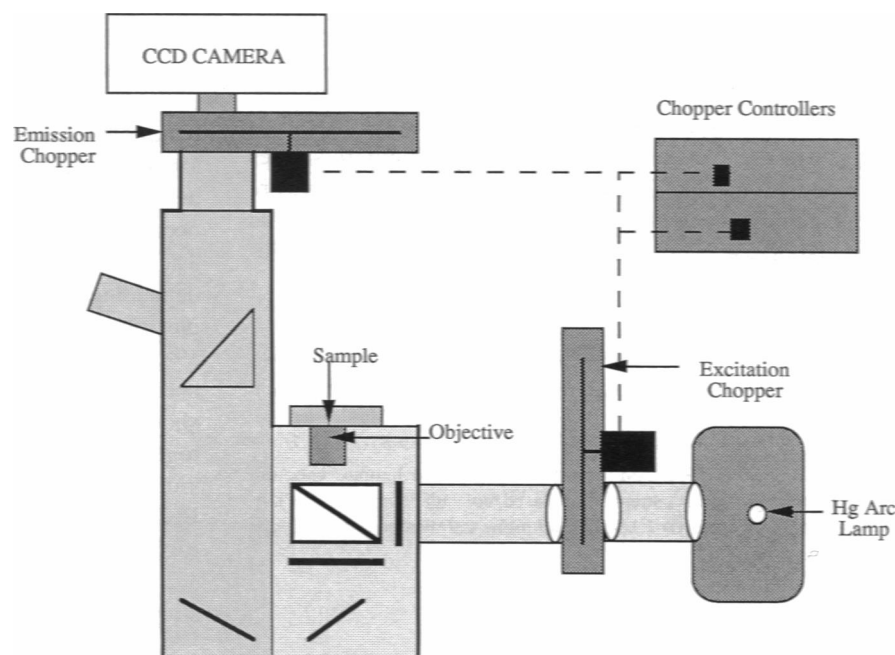
Immunohistochemistry

AX-2 cells grown to a density of 5×10^6 /ml in HL-5 medium at room temperature were washed with PB, plated onto a coverslip, and allowed to adhere for 30 min. After fixation in ice-cold methanol, cells were stained with a mouse monoclonal antibody against *Dictyostelium discoideum* myosin II (396) overnight, washed with PB, and treated with a 1/10 dilution of the biotinylated goat anti-mouse antibody for 2 h, then washed with PB, incubated with SBMC at a 1/5 dilution for 30 min, washed in PB-gelvatol, and sealed under a coverslip.

Time-resolved delayed luminescence image microscopy

The principles and operation of the TR-DLIM have been previously described (Marriott et al., 1991). In this work we used a Zeiss Axiocvert 35 microscope with the following modifications (Fig. 1). The collimated output of a voltage-stabilized 100-W mercury lamp was focused onto a two-sector excitation chopper (Model 221, HMS Electronic, Leverkusen, Germany)

FIGURE 1 Schematic diagram of the time-resolved light microscope (see text for further details). The excitation light was supplied by a voltage-regulated (Heinzinger, Rosenheim, Germany) 100-W mercury arc lamp (Zeiss, Oberkochen, Germany). The light was focused on a two-sector chopper blade with a condenser lens (Melles Griot, Holland) and then recollimated with a second identical condenser lens. After passage through a 340-nm interference filter, the chopped excitation beam was directed into the microscope body. The autofluorescence and sensitized europium ion signals were selected through a KV515 filter or an RG 600 filter. In-phase or out-of-phase images were recorded by an appropriate selection of the phase delay on the HMS 221A controller as described in the text. The sample image was then focused onto a Photometrics 200 series cooled CCD camera controlled by a Macintosh IIx computer.



that was open for 21.5% of the duty cycle. The chopped light was recombined and directed into the microscope body. A customized filter block was constructed to efficiently excite the bathophenanthroline group and collect the sensitized emission of the europium ion. The block consisted of a 340-nm interference filter, the FTTC dichroic mirror supplied by Zeiss and a bandpass filter which passed light beyond 510 nm (KV515), or beyond 600 nm (RG600). The emission chopper (model 221A, HMS) with a two-sector blade housed in a light-tight adapter, was open for 50% of the duty cycle. This chopper was phase-locked to the excitation chopper and positioned just before a cooled, charged coupled-device camera (Series 200, Photometrics, Tucson, AZ) which operated under the control of an Apple IIx computer. Images were collected by binning 2–4 pixels with an acquisition time of ~2–3 s. Prompt-fluorescence images were obtained by running the two choppers “in phase” at a defined frequency. Delayed luminescence images were recorded by running the choppers “out of phase” at the same frequency. The delay between the choppers was varied using the phase control dial on the HMS 221 controller.

Image processing

Images represented on the basis of the delayed luminescence lifetime were computed using a Fortran program running on a VAX computer (Digital Equipment Co., Maynard, MA). For a single exponential decay, the decay curve, $I = B + I_0 e^{-t/\tau}$, was transferred to its linearized form, $\ln(I - B) = \ln I_0 - t/\tau$, where I_0 is the initial intensity, I is the intensity at time t , τ is the lifetime of the delayed luminescence, and B is the system offset. In the curve fitting process, both parameters τ and B were searched simultaneously

to obtain a best fit based on the least squares principle. This method of linear fitting with double variables is more efficient and reliable than that used in Marriott et al. (1991); for example, for a sequence of eight images (100×100 pixels), the lifetime calculation was finished within seconds. A sequence of images collected with the two-sector choppers in a time interval of 210 μ s was analyzed using the linear curve fitting routine on a pixel-by-pixel basis. Delayed luminescence lifetime images were exported to the Macintosh IIx computer for further image processing with the public domain software package *National Institutes of Health Image*. The background pixels which present an intensity less than a certain value were assigned to a value of 255 on the 8-bit image scale, whereas the lowest lifetime value is set to 250 and the maximum lifetime value to 0 on this scale; i.e., a lifetime value τ ($\tau_{\min} \leq \tau \leq \tau_{\max}$, μ s) corresponds to an intensity of $I = 250 (\tau_{\max} - \tau)/(\tau_{\max} - \tau_{\min})$, or, an intensity value I , read in the 8-bit image scale, represents a lifetime of $\tau = \tau_{\max} - I(\tau_{\max} - \tau_{\min})/250$.

RESULTS

Validation of time-resolved measurements

In TR-DLIM, control experiments must be performed to show that images obtained in the out-of-phase condition are free of contributions from scattered light and prompt fluorescence (Marriott et al., 1991). Calibration of the reading on the phase-delay controller to the delay time was performed by imaging a prompt fluorescent sample (rhodamine labeled

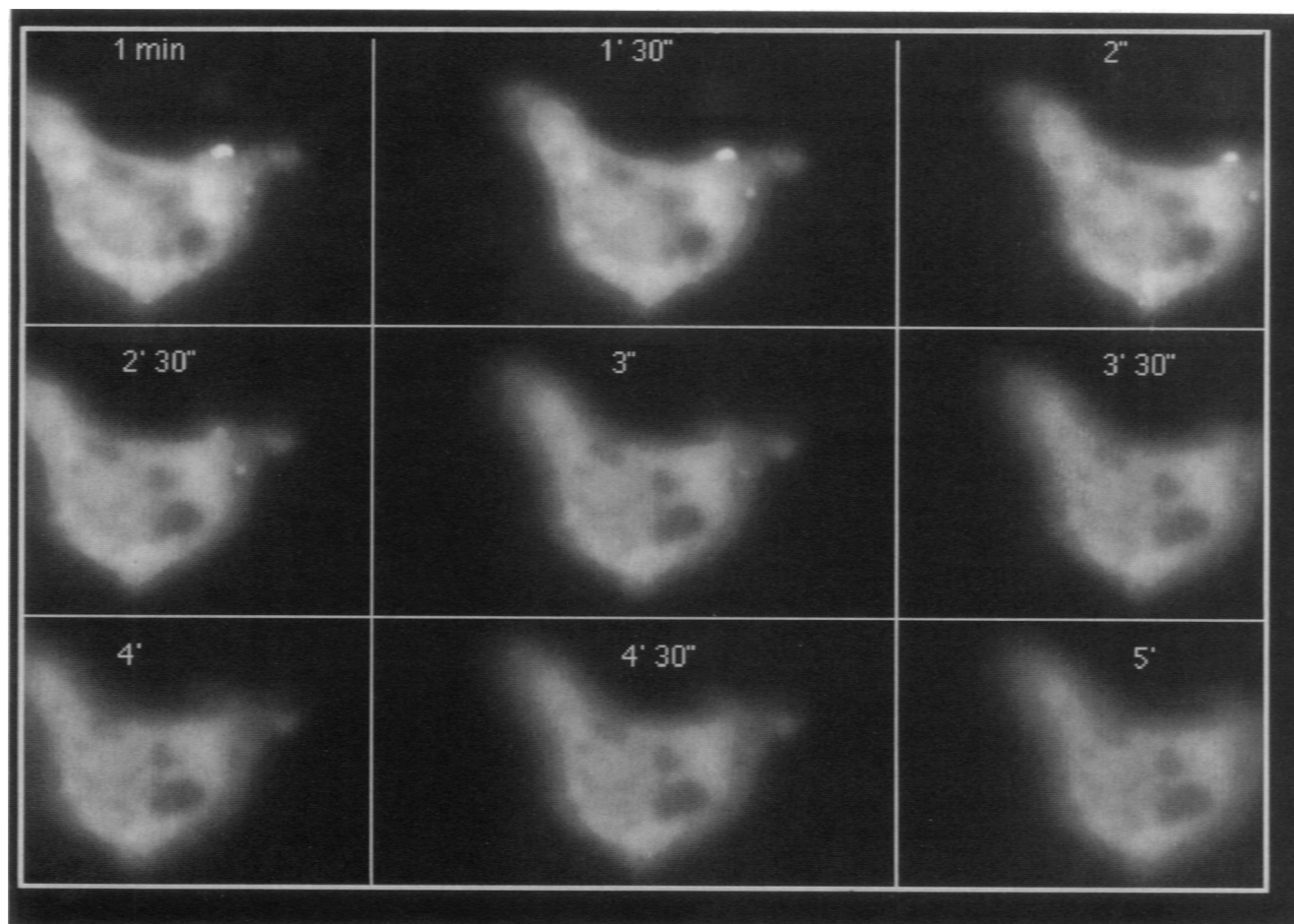


FIGURE 2 Effect of near ultraviolet irradiation on the steady-state luminescence intensity of SBMC. The fixed *D. discoideum* cell preparation labeled with the anti-myosin II antibody, biotinylated goat anti-mouse antibody, and the SBMC complex (0.06μ M) was irradiated continuously with 340-nm light. Images were recorded at the indicated times using a 2-s exposure; emission wavelength was selected through a KV 515 filter.

latex sphere) as a function of the phase delay reading. An image series was recorded over a phase reading of 20° until 100° at an interval of 10° using the two-sector chopper running at an excitation frequency of 169.5 Hz. The steady-state prompt fluorescence images were detected at the in-phase settings from 10° up to 25° , and ~ 80 – 100° of the next cycle, while the steady-state delayed luminescence images were obtained at the out-of-phase settings ~ 40 – 70° . We determined that a phase difference of 40° corresponds to 1.68 ms.

Photostability of the Eu^{3+} -SBMC complex

To examine the stability of SBMC toward excitation with near ultraviolet light we irradiated a myosin II labeled immunofluorescence preparation of amoeba cells stained with SBMC. Photobleaching of the preparation as a function of time was performed by imaging the steady-state emission of SBMC using 340 nm (10-nm bandpass) excitation delivered from a 100-W mercury arc lamp (Fig. 2). The emission recorded by the camera represents the sum of the steady-state prompt fluorescence background and delayed luminescence of SBMC. After 5 min of continuous irradiation the SBMC emission was still 68% of its original value. The relative insensitivity of SBMC to near-ultraviolet irradiation mediated photobleaching probably results from the very short lifetime of the excited singlet state of the BCPDA fluorophore which would tend to limit excited state reactions with molecular oxygen, the primary cause of photobleaching. On a far longer time scale we find SBMC-labeled fixed cell preparations stored in the refrigerator maintain their delayed fluorescence emission for at least one year.

Steady-state delayed luminescence imaging using SBMC

The large number of europium ion chelates in the SBMC generates a signal that is usually bright enough to image with

the naked eye without gated detection. The distribution of myosin II in the dividing *D. discoideum* cell shown in Fig. 3 was recorded using a 2-s exposure and an emission filter that selects for wavelengths greater than 600 nm. Despite the presence of a large autofluorescence signal the large separation in energy (about $13,000\text{ cm}^{-1}$) between the excitation (340 nm) and emission (612 nm) can be used to highlight the europium ion signal associated with the myosin II antibody, in this the cleavage furrow of the dividing cell. This large excitation-emission energy separation of the Eu^{3+} -BCPDA chelate is considerably greater than that found for organic-based fluorophores which is typically 1000 – 3000 cm^{-1} and rarely exceeds 8000 cm^{-1} (Weber and Farris, 1978).

Time-resolved delayed luminescence imaging using SBMC

Images of a *D. discoideum* cell double-labeled with a prompt fluorescent DNA stain ($1\text{ }\mu\text{M}$ ethidium homodimer) and a biotinylated antibody against myosin labeled with SBMC (60 nM streptavidin) are represented in terms of steady-state prompt fluorescence emission (in phase, Fig. 4 A), delayed luminescence emission (out of phase, Fig. 4 B), and the phase-contrast image (Fig. 4 C). The in-phase image, i.e., all of the prompt fluorescence and part of the delayed fluorescence emission, does not reveal any distinctive structure in the cell on the left-hand side of the image, the main signal contributions originate from cellular autofluorescence; the image of the right-hand cell is dominated by a signal from ethidium homodimer staining of an out-of-focus nucleus. When the same cells are imaged in the out-of-phase mode, the background prompt fluorescence emissions are completely suppressed, revealing the delayed luminescence of SBMC-labeled myosin II whose distributed is primarily restricted to the cell cortex and the plasma membrane in agreement with earlier results of Yumura et al. (1984).

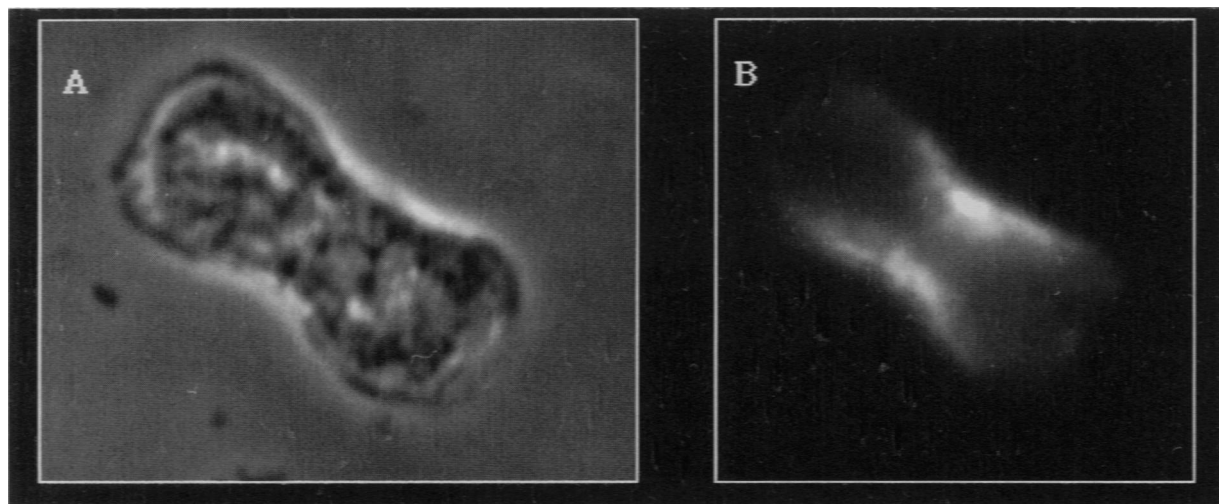


FIGURE 3 Phase-contrast and steady-state luminescence image of a fixed *D. discoideum* cell undergoing mitosis. The sample was prepared as described in Fig. 2 and irradiated under steady-state illumination conditions using 340-nm light; the emission was collected over 2 s through the RG600 filter.

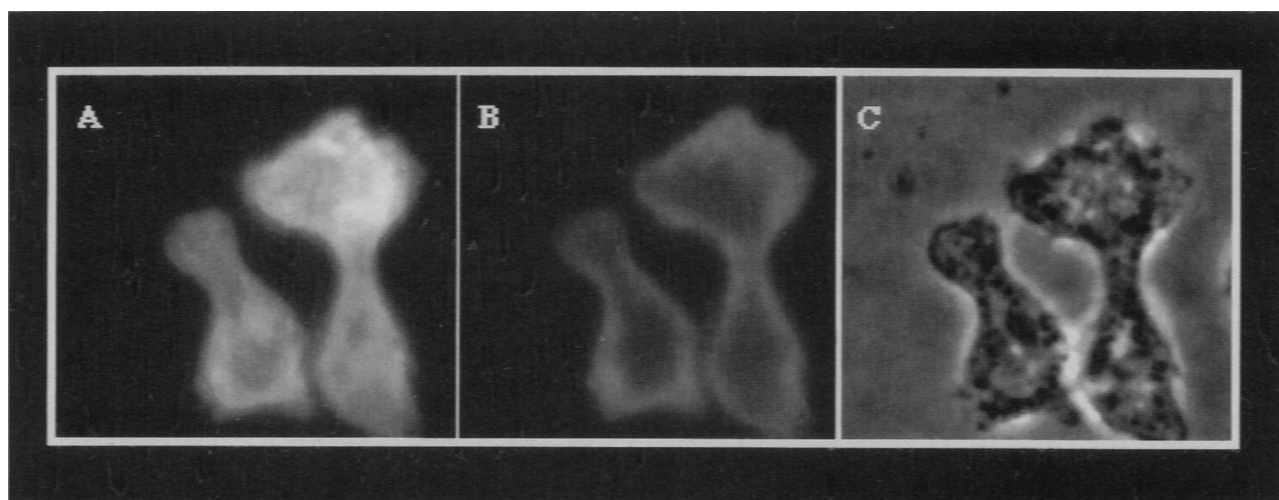


FIGURE 4 Images of a *D. discoideum* cells double-labeled with ethidium homodimer ($1\ \mu\text{M}$) and a biotinylated antibody against myosin, which was in turn labeled with SBMC at a 1/5 dilution ($0.06\ \mu\text{M}$ streptavidin). (A) Steady-state prompt fluorescence emission (in phase). (B) Delayed luminescence fluorescence emission (out of phase). (C) Phase-contrast image. The cell on the right-hand side shows an ethidium homodimer-stained nucleus which is slightly out of focus.

The delayed luminescence image shown in Fig. 4 were obtained with a modest amount of near ultraviolet illumination (21.5% output of 343-nm line of a 100-W mercury lamp) using an acquisition time of 2 s, which compares well with image acquisition times we commonly use with prompt fluorescent probes in fixed cells such as those based on Prodan (Weber and Farris, 1979). On a mole-for-mole basis, the delayed luminescence signal obtained with SBMC is much stronger than the triplet-state phosphorescence of eosin or acridine orange (Marriott et al., 1991).

Imaging the distribution of Con A in oxygenated living cells using delayed luminescence emission

Con A binds to cell surface glycoproteins of *D. discoideum* cells, whereupon in an energy-dependent and oxygen-requiring process (Jay and Elson, 1992), it aggregates on the cell surface, translocates to the cell anterior, and is capped. Imaging the distribution of membrane proteins in *D. discoideum* cells is complicated by strong autofluorescence signals, primarily from pinocytosed vesicles. To show the effectiveness of TR-DLIM in removing unwanted background signals, we used SBMC to image the distribution of biotinylated Con A in cells containing an extremely large prompt fluorescence signal originating from pinocytosed lucifer yellow. Both probes were excited with 340-nm light and the emission was collected through a KV 515 cutoff filter (Schott Glas, Darmstadt, Germany). The in-phase image (Fig. 5 A) is dominated by the prompt fluorescence signal of lucifer yellow, which obscures the delayed emission of SBMC labeled Con A. The image shown in Fig. 5 B was collected at the border of in-phase and out-of-phase setting, the lucifer yellow emission is almost rejected, and, as expected, in the out-of-phase images (Fig. 5, C–E), the lucifer yellow emission is completely rejected, revealing the delayed emission

of capped SBMC-Con A. Shortly after addition of the SBMC to the cells, the delayed emission from SBMC was uniformly distributed around the cell (data not shown). The power of TR-DLIM to improve image contrast can be appreciated in Fig. 5, C–E, in which the membrane surrounding the pinocytosed vesicle is visible through the delayed luminescence of SBMC labeled Con A. The intense staining from the lucifer yellow (Fig. 5 A) smears over a much larger pixel area than the vesicle defined by the Con A membrane envelope (Fig. 5, B–E). This study also shows the SBMC probe can use TR-DLIM to record images of living cells in oxygenated buffers. This solvent condition is incompatible with TR-DLIM studies that employ triplet-state-based emission probes such as eosin or acridine orange (Marriott et al., 1991).

Representation of images based on delayed luminescence decay time

Validation of delayed luminescence lifetime determinations in the microscope was shown by comparing macroscopic and microscopic emission decay times of a $0.30\ \mu\text{M}$ solution of the SBMC in phosphate buffer. An image sequence representing the time-dependent decay of this SBMC solution is shown in Fig. 6 A. The images were collected from $210\ \mu\text{s}$ to $1680\ \mu\text{s}$, with a time delay of $210\ \mu\text{s}$ between each image. Calibration of the chopper control module from phase-delay to time-delay scale was performed as described in the Materials and Methods section. The decay rate in each of the 100×100 image pixels was calculated through a first order curve fitting based on the least-squares solution to overdetermined linear systems. The lifetime image is shown in Fig. 6 B; the mean value of the lifetime distribution is about $740\ \mu\text{s}$, with a half-bandwidth of $\sim 80\ \mu\text{s}$ (Fig. 6 C). The same SBMC solution was measured simultaneously in

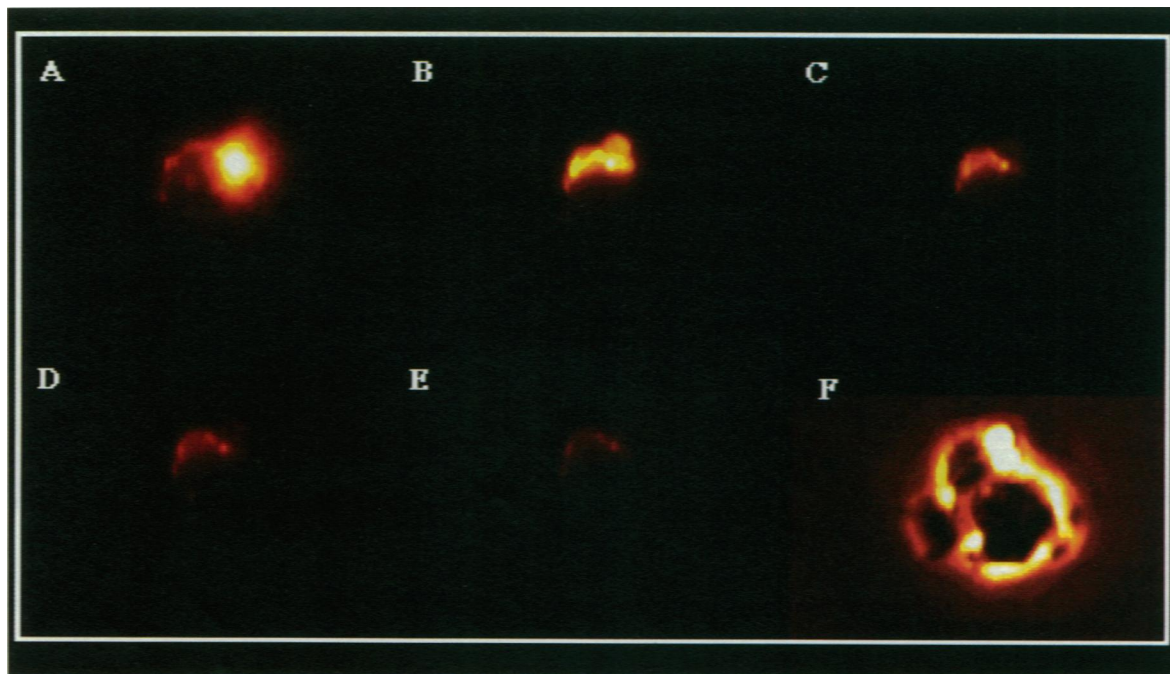


FIGURE 5 Images of the capping of biotinylated Con A on the surface of living *D. discoideum* amoebae containing a signal strong prompt fluorescence from pinocytosed lucifer yellow. (A) In-phase image, phase angle 20°. (B) Image collected on the border of in-phase and out-of-phase, 30°. (C) Out-of-phase image, phase angle 40°. (D) Out-of-phase, 50°. (E) Out-of-phase, 60°. (F) Phase contrast image. Each image was acquired for 2 s; the pinocytosed vesicle underwent some motility during the image sequence acquisition time.

SLM-AB2 luminescence spectrophotometer (SLM-Aminco, Urbana, IL) using 340-nm excitation and 612-nm emission. The intensity decay versus time is shown in Fig. 6 D, together with a fitted curve for a single exponential decay of 745 μ s, which agrees well with the mean value obtained from the microscope measurement. Although the temporal resolution of the microscope-based lifetime determination is much lower than the AB2 instrument, which has a resolution of 2 μ s, the 10,000 independent determinations of the decay time clearly improve the statistics of the measurement and result in an accurate determination of the average lifetime. Lifetime measurements are of course possible with a larger pixel array; for our camera, we can perform up to 1.4×10^6 independent lifetime determinations. In a control experiment we have shown that near-ultraviolet excitation of free europium ion up to a concentration of 3.9 mM does not result in any significant delayed luminescence signal.

TR-DLIM was also performed on BCPDA-Eu³⁺-labeled dextran beads in phosphate buffer (data not shown). The delayed emission lifetime of BCPDA on the bead was centered at 450 μ s with a bandwidth of about 60 μ s. The differences in the lifetime of Eu³⁺-BCPDA in phosphate buffer (210 μ s; Gudgin Templeton and Pollak, 1989), covalently attached to aminodextran in phosphate buffer (450 μ s), and in the SBMC in phosphate buffer (745 μ s) are probably related to the relative amount of the 1:1 and 1:2 BCPDA-Eu³⁺ complex and the participation of other ligands from the protein or aminodextran which would presumably reduce the number of water or phosphate ion ligands, thereby increasing the radiative decay time (Gudgin Templeton and Pollak, 1989).

Gated emission detection and lifetime imaging can also be applied to immunofluorescence specimens as shown for Eu³⁺-SBMC-labeled myosin II antibody in *D. discoideum* (Fig. 7). A rather broad lifetime distribution was calculated from the image series (Fig. 7 B). Inspection of the lifetime image suggests the longer lifetime distribution appears to follow that of membrane-associated myosin, whereas the cytoplasmic form has the shorter lifetime distribution which appears red to black in this image (Fig. 7 B). The range of the lifetime distribution for this preparation is much shorter than that found for SBMC in solution (740 μ s); this may be result of competing ligands added during the fixation process which may reduce the number of 1:2 Eu³⁺-BCPDA species, thereby decreasing the radiative decay time.

DISCUSSION

The bathophenanthroline-based chelate forms a stable complex with the europium ion with a half-life that is sufficiently long to guarantee that no dissociation occurs during the course of the experiment. Unlike the chelate described by Seveus et al. (1992), the Eu³⁺-BCPDA complex is stable toward the excitation levels commonly used in fluorescence microscopy. Upon excitation of the Eu³⁺-BCPDA chelate with near ultraviolet light, a highly efficient energy transfer process occurs which sensitizes europium ion emission at 612 nm with an emission lifetime in solution of 210 μ s for the 1:1 Eu³⁺-BCPDA complex in PB and 770 μ s for the 1:2 Eu³⁺-BCPDA complex (Gudgin Templeton and Pollak, 1989), 450 μ s in a BCPDA-dextran complex in PB, and 745 μ s for the SBMC complex in PB. On the basis of this lifetime

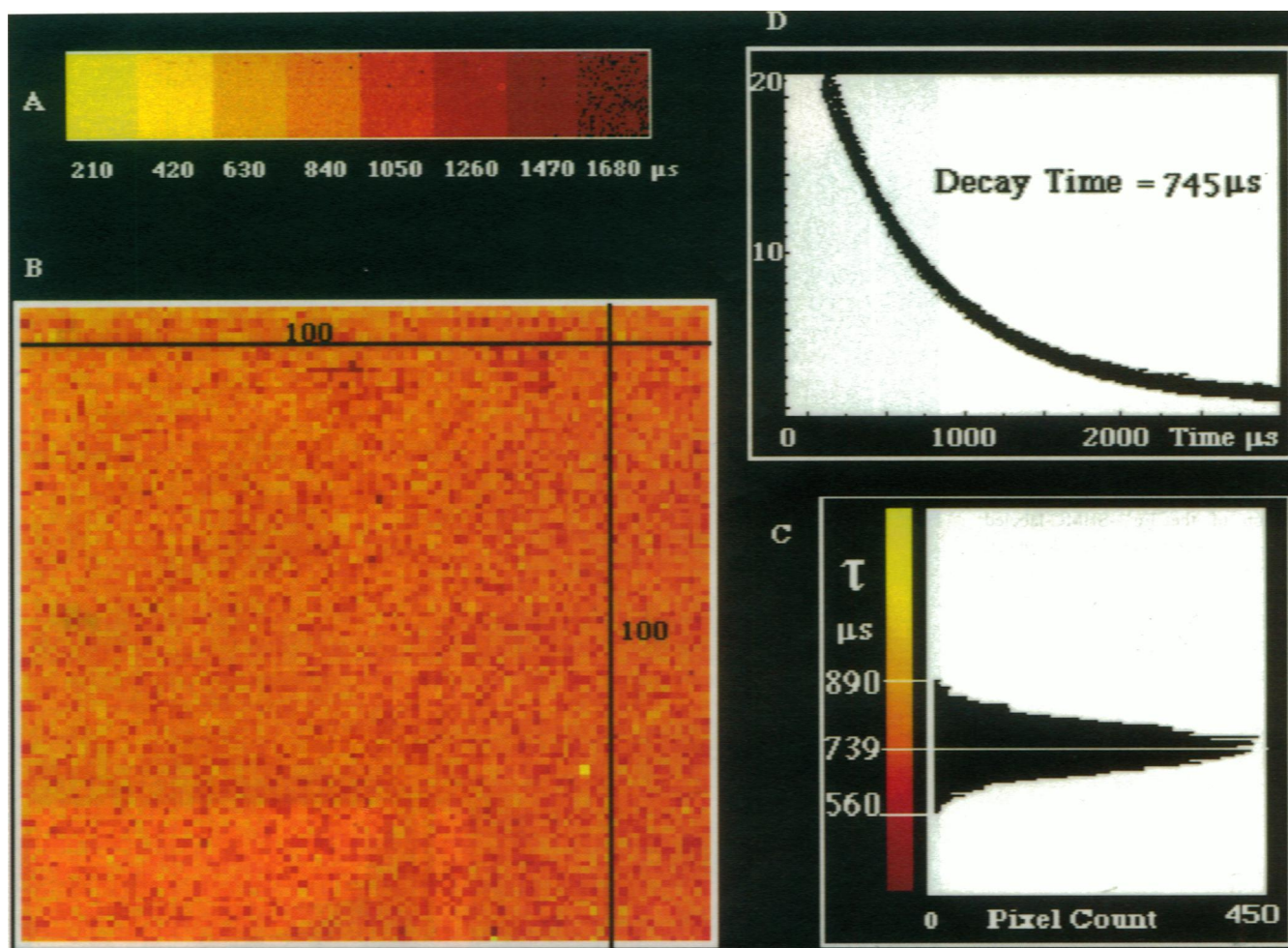


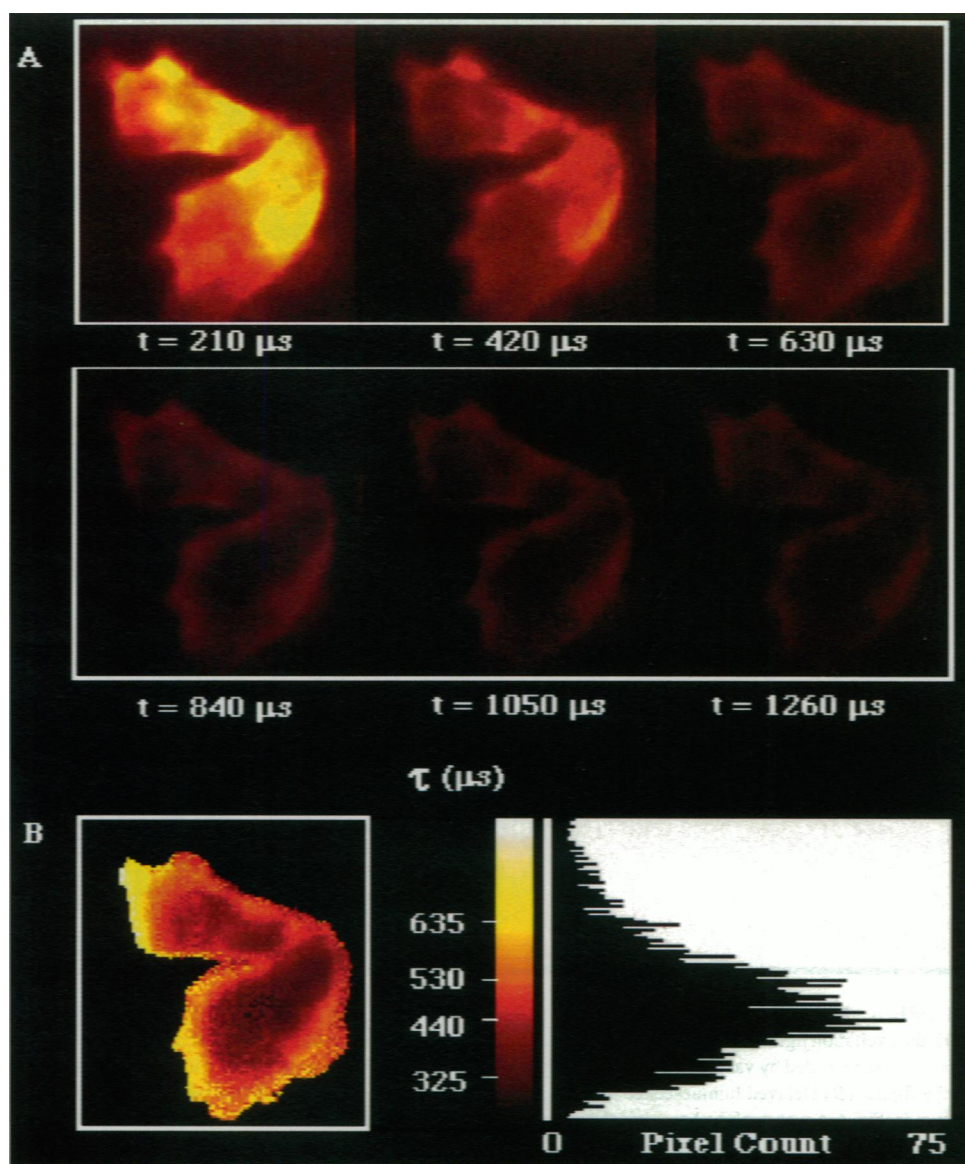
FIGURE 6 Microscope based lifetime imaging of the SBMC complex. (A) 20 μl of an 0.3 μM SBMC solution in PB was placed on a microscope coverslip. Periodic excitation light at 169.5 Hz collected through a 340-nm interference filter was focused on the surface of the coverslip. Time-resolved delayed emission images were recorded by varying the phase of the phase-locked excitation chopper. The emission was collected through an RG600 filter at the times indicated in the figure. (B) Delayed luminescence lifetime image of the SBMC in a 100×100 pixel array; the time-dependent intensity decay of the SBMC images shown in Fig. 6 A was analyzed on a pixel-by-pixel basis in terms of a single exponential decay. (C) Distribution of the lifetime of SBMC vs. pixel count obtained from Fig. 6 B; it follows a narrow Gaussian distribution with a mean value of 739 μs and a deviation of about 80 μs . (D) The intensity decay of the same stock SBMC sample (400 μl) measured in SLM Aminco AB2 luminescence spectrometer. Excitation at 340 nm (8 nm bandwidth) and emission at 612 nm (8 nm bandwidth). The 6- μs pulse was delivered at a frequency of 100 Hz. Emission was collected from 100 μs to 3 ms. The data were fitted to a single exponential curve with a decay rate of 745 μs .

study we suspect emission from the 1:2 Eu^{3+} -BCPDA complex is dominant in the SBMC. In our studies with fixed and living cells we used phosphate buffer, which is reported to have a quenching effect on the europium luminescence (Gudgin Templeton and Pollak, 1989). The emission lifetime of SBMC does not change significantly when PB is replaced by Tris as a buffer, which indicates that the europium ion is primarily in the form of the 1:2 Eu^{3+} -BCPDA complex, a conclusion consistent with the macroluminescence lifetime of SBMC reported in Fig. 6. However, buffers can influence the emission lifetime of the Eu^{3+} -BCPDA if they replace water as co-ligands or else disrupt the 1:2 Eu^{3+} -BCPDA. We consistently find shorter lifetimes of SBMC in fixed and living cells, which suggests a breakdown of 1:2 Eu^{3+} -BCPDA species in these complex molecular environments.

The SBMC label has some attractive features which lends itself for light microscopical studies of cell structure and

dynamics. For example, we have shown that the delayed luminescence quantum yield of the SBMC complex is high enough to image the distribution of Con A molecules on the plasma membrane of amoeba cells, perhaps 10^6 molecules. The sensitized europium ion emission rapidly depopulates the excited singlet state of the BCPDA fluorophore, thereby reducing diffusion-limited photobleaching reactions. This property allows images to be acquired with long exposure times, although for the measurements made in this report, only relatively low doses of near ultraviolet irradiation were found necessary to obtain high contrast images. In most of the time-resolved immunofluorescence preparations we report here the SBMC concentration was 60 nM in streptavidin, comparable with the streptavidin concentration used with prompt fluorescent based immunofluorescence studies. SBMC can be used to resolve fine structure in immunofluorescence labeling of myosin II, suggesting that its large

FIGURE 7 Gated emission images, lifetime image, and histogram distribution of the Eu^{3+} -SBMC-labeled anti-myosin II in a *D. discoideum* cell prepared in a similar manner to that described in Fig. 2. The mean emission lifetime of SBMC within the cell is 426 μs and that associated with the membrane is 514 μs .



molecular size does not restrict its diffusion within the cell. Finally, the streptavidin-based reagent can be applied to study the distribution of numerous ligands, proteins, and DNA labels which contain biotin as a molecular marker.

The increasing application and development of microscope-based detection of molecules in cellular and molecular biology owes a great deal to the introduction of solid-state imaging cameras and new luminescent probes. However, although it is possible to record images in vitro of single actin filaments containing less than a hundred molecules of rhodamine phalloidin (Harada et al., 1990), this level of detection is rarely achieved in studies using living or fixed cells because of a significant signal contribution from cellular autofluorescence. For some cells such as *Dictyostelium* amoebae, this background signal is equivalent to several thousand fluorescein molecules (unpublished observations). The application of BCPDA chelates to TR-DLIM has allowed us to obtain high-contrast images of specific molecules in fixed cells or in highly autofluorescent living cells

such as *D. discoideum*. As shown in Fig. 4, the steady-state prompt fluorescence signal of lucifer yellow is more than 100 times that of the steady-state delayed luminescence of the SBMC label. It is unlikely that this degree of probe resolvability could be achieved in the fluorescence microscope using only spectral discrimination methods; in fact, we have shown that delayed luminescence imaging permits a discrimination against prompt fluorescence signals by up to 7 orders of magnitude (Marriott et al., 1991). The ability of TR-DLIM to completely suppress autofluorescence, prompt fluorescence of extrinsic probes, and Rayleigh and Raman scatter should be useful in imaging molecules present in low copy number and in immunofluorescence studies of naturally fluorescent cells such as photosynthetic algae.

We believe that certain chemical modifications to the structure of BCPDA will lead to an improvement in its quantum yield and extinction coefficient of the chelate which in turn will allow the sensitivity of TR-DLIM to reach that level presently enjoyed by fluorescence microscopy. One area we

are interested in pursuing is to improve the chelating capability of the BCPDA group; BCPDA is capable of chelating only four of the nine ligation sites. The remaining ligands are probably water molecules, although in the SBMC complex most europium ions probably share two BCPDA ligands.

This work was supported in part by a grant from the Deutsche Forschungsgemeinschaft (Ma 1499/1).

REFERENCES

- Beverloo, H. B., van A. Schadewijk, J. Bonnet, van der R. Geest, R. Runia, N. P. Verwoerd, J. Vrolijk, J. S. Ploem, and H. J. Tanke. 1992. Preparation and microscopic visualization of multicolor luminescent immunophosphors. *Cytometry*. 13:561–570.
- Diamandis, E. P., and R. C. Morton. 1988. Time-resolved fluorescence using a europium chelate of 4:7-bis(chlorosulfonyl)-1,10-phenanthroline-2,9-dicarboxylic acid (BCPDA). *J. Immunol. Methods*. 112:43–52.
- Evangelista, R. A., A. Pollak, B. Allore, E. F. Templeton, R. C. Morton, and E. P. Diamandis. 1988. A new europium chelate for protein labeling and time-resolved fluorometric applications. *Clin. Biochem.* 21:173–178.
- Gudgin Templeton, E. F., and A. Pollak. 1989. Spectroscopic characterization of 1:10-phenanthroline-2,9-dicarboxylic acid and its complexes with europium. III: Luminescent europium chelates useful for analytical applications in aqueous solution. *J. Lumin.* 43:195–205.
- Harada, Y., K. Sakurada, T. Aoki, D. D. Thomas, and T. Yanagida. 1990. Mechanochemical coupling in actomyosin energy transduction studied by in vitro movement assay. *J. Mol. Biol.* 216:49–68.
- Jay, P. Y., and E. L. Elson. 1992. Surface particle transport mechanism independent of myosin II in dictyostelium. *Nature*. 356:438–440.
- Lief, R. C., and L. M. Vallarino. 1991. Rare-earth chelates as fluorescent markers in cell separation and analysis. *Cell Separation Science and Technology*, ACS Symposium. 464:41–58.
- Marriott, G., R. M. Clegg, D. J. Jovin, and T. M. Jovin. 1991. Time resolved imaging microscopy: phosphorescence and delayed fluorescence imaging. *Biophys. J.* 61:1374–1387.
- Morton, R. C., and E. P. Diamandis. 1990. Streptavidin-based macromolecular complex labeled with a europium chelate suitable for time-resolved fluorescence immunoassay applications. *Anal. Chem.* 62:1841–1845.
- Saha, A. K., K. Kross, E. D. Kloszewski, D. A. Upson, J. L. Toner, R. A. Snow, C. D. V. Black, and V. C. Desai. 1993. Time resolved fluorescence of a new europium chelate complex: demonstration of highly sensitive detection of protein and DNA samples. *J. Am. Chem. Soc.* 115: 11032–11033.
- Seveus, L., M. Visala, S. Syrjanen, M. Sandberg, A. Kuusisto, R. Harju, J. Salo, I. Hemmila, H. Kojola, and E. Soini. 1992. Time-resolved fluorescence imaging of europium chelate label in immunohistochemistry and in situ hybridization. *Cytometry*. 13:329–338.
- Weber, G., and F. J. Farris. 1979. Synthesis and spectral properties of a hydrophobic fluorescent probe: 6-propionyl-2-(dimethylamino)naphthalene. *Biochemistry*. 18:3075–3078.
- Yumura, S., H. Mori, and Y. Fukui. 1984. Localization of actin and myosin for the study of amoeboid movement in dictyostelium using improved immunofluorescence. *J. Cell Biol.* 99:894–899.